ARTICLE

ACS chemical biology

Targeted Delivery of Antigen Processing Inhibitors to Antigen Presenting Cells *via* Mannose Receptors

Eun-Ang Raiber[†], Calogero Tulone[‡], Yanjing Zhang[‡], Luisa Martinez-Pomares[§], Emily Steed[‡], Anna M. Sponaas[∥], Jean Langhorne[∥], Mahdad Noursadeghi[‡], Benjamin M. Chain[‡,⊥,*], and Alethea B. Tabor[†,⊥,*]

[†]Department of Chemistry, UCL, London, U.K., [‡]Division of Infection and Immunity, UCL, London, U.K., [§]School of Molecular Medical Sciences, University of Nottingham, U.K., and [∥]Division of Parasitology, National Institute for Medical Research, London, U.K. [⊥]These authors have contributed equally to this work.

ABSTRACT Improved chemical inhibitors are required to dissect the role of specific antigen processing enzymes and to complement genetic models. In this study we explore the *in vitro* and *in vivo* properties of a novel class of targeted inhibitor of aspartic proteinases, in which pepstatin is coupled to mannosylated albumin (MPC6), creating an inhibitor with improved solubility and the potential for selective cell tropism. Using these compounds, we have demonstrated that MPC6 is taken up *via* mannose receptor facilitated endocytosis, leading to a slow but continuous accumulation of inhibitor within large endocytic vesicles within dendritic cells and a parallel inhibition of intracellular aspartic proteinase activity. Inhibition of intracellular proteinase activity is associated with reduction in antigen processing activity, but this is epitope-specific, preferentially inhibiting processing of T cell epitopes buried within compact proteinase-resistant protein domains. Unexpectedly, we have also demonstrated, using quenched fluorescent substrates, that little or no cleavage of the disulfide linker takes place within dendritic cells. This does not appear to affect the activity of MPC6 as an inhibitor of cathepsins D and E *in vitro* and *in vivo*. Finally, we have shown that MPC6 selectively targets dendritic cells and macrophages in spleen *in vivo*. Preliminary results suggest that access to nonlymphoid tissues is very limited in the steady state but is strongly enhanced at local sites of inflammation. The strategy adopted for MPC6 synthesis may therefore represent a more general way to deliver chemical inhibitors to cells of the innate immune system, especially at sites of inflammation.

Antigen presenting cells (including dendritic cells (DC) and macrophages) are equipped with an array of membrane and cytoplasmic receptors known as pattern recognition receptors (PRR), with which they bind to microbial components (pathogen associated molecular patterns, PAMPs). Once internalized, any PAMP-associated proteins are subject to regulated proteolysis (the exogenous antigen processing pathway), producing peptides that bind to class II major histocompatibility complex (MHC) receptors and hence stimulate T cell adaptive immunity (*1*). The interaction between antigen presenting cell and T cell is widely recognized as being one of the key steps regulating both the magnitude and the type of immune response. The experimental manipulation of antigen presenting cells, either to enhance therapeutic and protective responses or to inhibit pathogenic responses, is therefore an important goal of applied immunology. Efficient delivery of such immunomodulators is one limiting factor in achieving this goal.

A number of studies have used antibodies to deliver antigens to antigen presenting cells *in vitro* or *in vivo* (*2*). This has achieved some significant successes. However, a wealth of experience from the field of tumor biology has shown that delivery of drugs *via* antibody conjugates poses formidable technical problems. An alternative approach is to target DC using ligands of lectins such as mannose receptors, themselves a family of PRRs (*3, 4*). We have explored this targeting strategy in the context of using the selective inhibitor pepstatin **1** to identify the role of aspartic proteinases cathepsins D and E in the proteolysis of antigen (*5, 6*). Pepstatin itself is a very potent inhibitor ($IC_{50} < 1$ nM for both cathepsins D and E). However, pepstatin is almost completely

*Corresponding authors, a.b.tabor@ucl.ac.uk, b.chain@ucl.ac.uk.

Received for review July 21, 2009 and accepted March 29, 2010.

Published online March 29, 2010

10.1021/cb100008p

insoluble in aqueous solution, and its peptidic nature gives very poor cell penetration. As a result, it is typically used at 10−100 μM *in vitro*, concentrations at which it rapidly forms crystalline deposits in tissue culture. In addition to improving its solubility, selective cellular targeting of pepstatin is desirable, since cathepsin D deficiency is known to result in profound neurotoxicity (*7*).

Our previous work addressed these issues by designing a mannose−pepstatin conjugate, MPC6 **2** (Figure 1, panel a) in which pepstatin is coupled to neomannosylated bovine serum albumin (BSA) *via* a disulfide linker. These initial studies confirmed that this strategy resulted in an inhibitor with increased solubility, which could inhibit processing of a model antigen ovalbumin (OVA) by bone marrow derived GM-CSF DC. However, only one T cell response was examined, and no information was available on uptake, intracellular distribution, and cell targeting of MPC6. The purpose of this study was to synthesize fluorescently labeled derivatives of MPC6 and to follow uptake, endocytosis, and processing of MPC6 by DC.

RESULTS AND DISCUSSION

Synthesis of Fluorophore-Labeled Analogues of MPC6. Fluorophore-labeled analogues of MPC6 were prepared using a modification of the approach that we have previously reported (*5*). Starting from the key intermediate **3**, the *tert*-butyloxycarbonyl (Boc) protecting group was removed, and the resulting free amine was coupled to the activated *N*-hydroxysuccinimide (NHS) ester of pepstatin (*5*) to give **4** (Figure 1, panel b). Removal of the 9-fluorenylmethyloxycarbonyl (Fmoc) group, followed by conversion to the iodoacetamide and coupling to neomannosylated BSA **5** gave MPC6-32 **6**. For the second monolabeled analogue, selective removal of the Fmoc group from **3** and coupling to pepstatin-NHS gave **7**, which was again deprotected, converted to the iodoacetamide, and coupled to neomannosylated BSA to give MPC6-40 **8**. Two probes were prepared with fluorophores in different positions relative to the disulfide bond, in order to investigate whether disulfide bond cleavage took place after uptake of MPC6 and the site and timing of such cleavage (*8*). In MPC6-32 **6**, the tetramethylrhodamine (TMR) label is placed on the mannose-BSA conjugate side of the disulfide bond. If the disulfide linker is cleaved, for example, by intracellular reduction, the label should remain with the mannose-BSA conjugate. Conversely, in MPC6-40 **8**, the TMR label is placed on the side of the pepstatin and should therefore remain with the inhibitor after cleavage of the disulfide linker. Measurements of TMR: BSA ratios by light absorption spectroscopy gave yields of around 1 TMR for every 2−3 BSA molecules. However, no remaining free thiol group could be detected by the Ellman test on either inhibitor. These results are consistent with many previous studies showing that only 30−50% of serum albumin molecules contain a reactive free thiol group, with the cysteine residue in the remainder in the form of mixed disulfides or oxidized to sulfenic and sulfonic acids and hence unreactive to iodoacetamides (*9*). Additionally, the BSA free sulfhydryl is buried within a hydrophobic site and is thus less accessible for reaction with iodoacetamides (*10*), also rendering the Ellman's test less reliable for measuring successful conjugation (*11*).

Uptake and Retention of MPC6 Analogues within DC. The binding/uptake of MPC6-32 **6** and MPC6-40 **8** by DC were first investigated by flow cytometry. Mouse DC can be isolated and/or differentiated *in vitro* following a number different protocols. *In vitro* culture of bone marrow precursors in GM-CSF gives rise to a population of cells that is 60−90% CD11c positive, with the remaining cells mostly immature DC precursors. MPC6-32 **6** (Figure 2, panel a) and MPC6-40 **8** (Supplementary Figure 1) are both taken up selectively by the CD11c positive fraction of cells. Uptake by DC is both dose- and time-dependent (Figure 2, panel b). The rate of uptake is slow and continues to increase over 18 h, the longest time period tested (Figure 2, panel c). The rate does not saturate over the range of concentrations tested at early time points, suggesting a low affinity interaction facilitates uptake. However, concentration-dependent saturation is observed at longer time points (Figure 2, panel c), suggesting that there is a maximum amount of inhibitor that can be taken up by each cell.

An alternative protocol for DC differentiation is to expand precursor cells in the growth factor Flt3L. This protocol produces a population that is almost entirely CD11c positive but can be subdivided into two subpopulations, expressing high and low levels of CD11b (*12*). Although both populations were able to take up MPC6-32 **6** (and MPC6-40 **8**, Supplementary Figure 2), the CD11b high population was more efficient (Figure 2, panel d), consistent with the fact that this population is believed to play the major role in uptake and processing

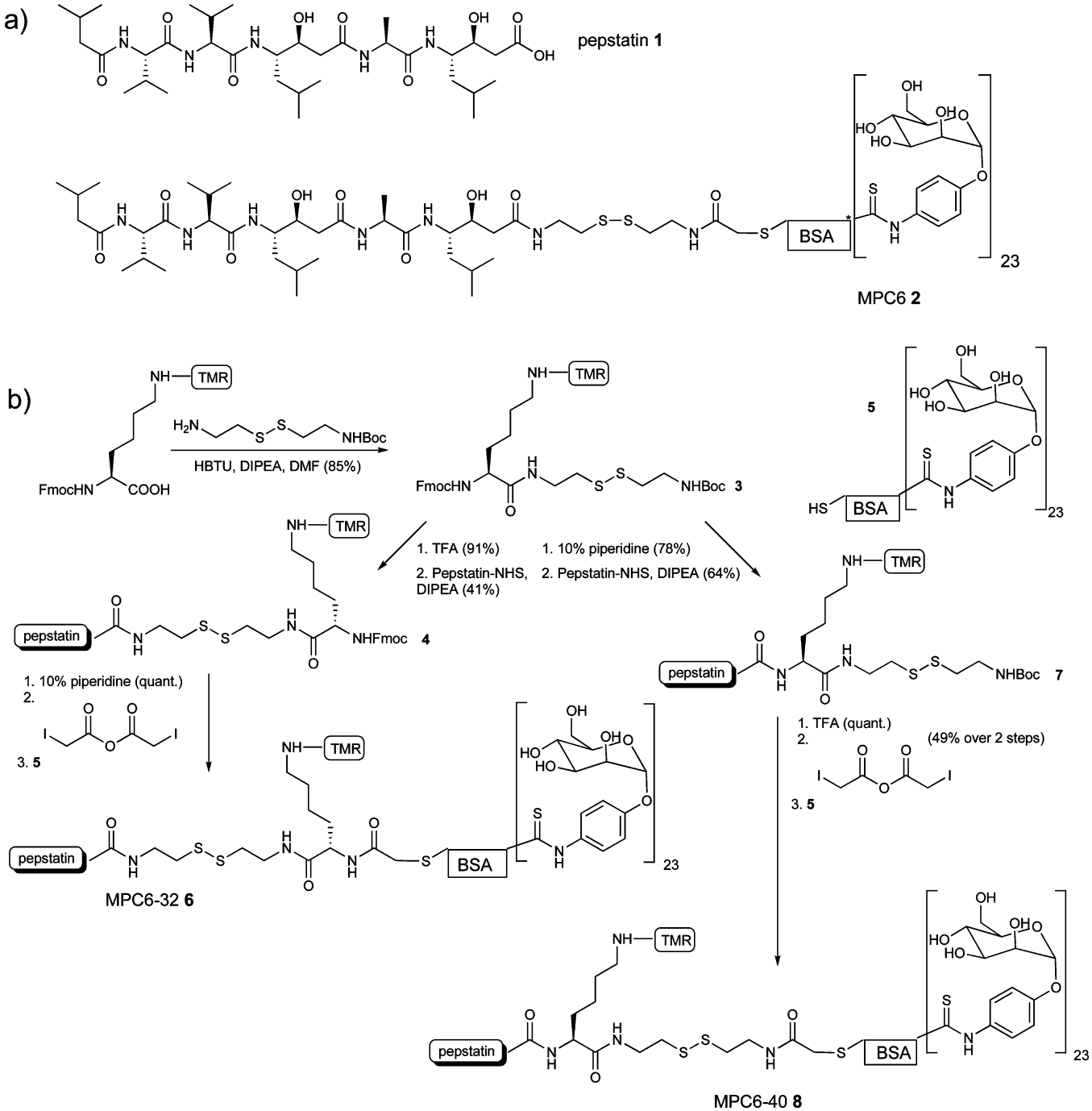

Figure 1. Chemical structure and synthesis of fluorescent derivatives of mannose pepstatin conjugates. a) Structures of pepstatin 1 **and MPC6** 2**. b) Scheme showing synthetic route to MPC6-32** 7 **and MPC6-40** 10**. TMR, tetramethylrhodamine; Fmoc, 9-fluorenylmethyloxycarbonyl; Boc, *tert*-butyloxycarbonyl; TFA, trifluoroacetic acid.**

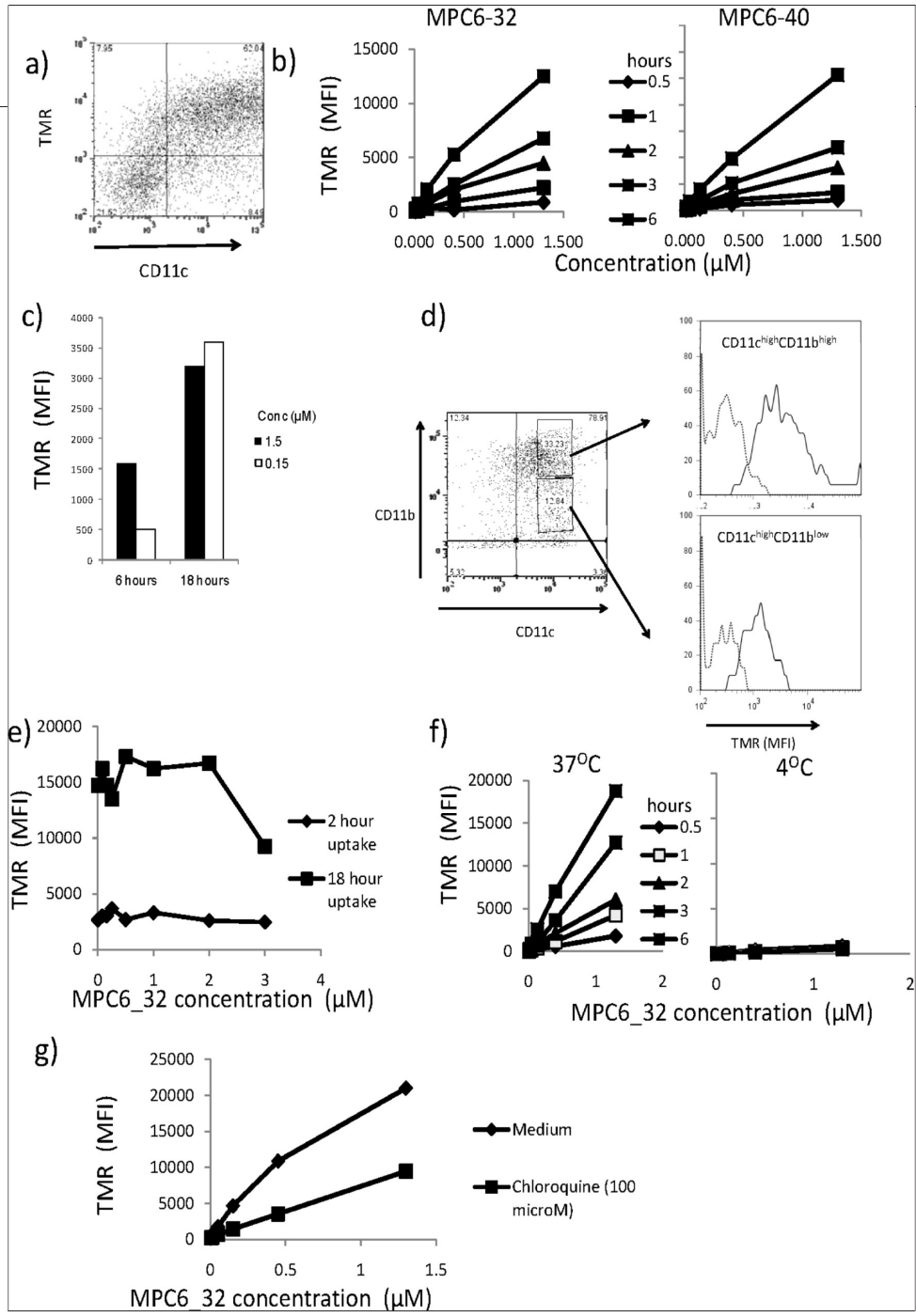

Figure 2. Uptake of MPC6 by DC *in vitro* analyzed by flow cytometry. Graphs show median fluorescent intensity (MFI) in the TMR channel. a) Uptake of MPC6-32 by GM-CSF bone marrow derived DC *in vitro*. b) GM-CSF bone marrow derived DC were incubated for different times and with different concentrations of MPC6-32 (left panel) or MPC6-40 (right panel) c) As for panel b, showing staining after 6 and 18 h (overnight) incubation at two concentrations of MPC6. d) Uptake of MPC6-32 by Flt3L bone marrow derived DC *in vitro*. The left panel shows the two CD11c DC populations. The right panels show TMR staining in cells incubated with (solid line) or without (dotted line) MPC6-32. e) Efflux of MPC6-32 from DC. GM-CSF bone marrow derived DC (5×10^4) were cultured for 2 or 18 h at 37 °C with MPC6-32 (0.5 μM) and then cultured for varying times in the absence of exogenous MPC6-32, before fixation. f) Flt3L bone marrow derived DC were incubated with MPC6-32 at 37 °C (left panel) or 4 °C (right panel). g) GM-CSF bone marrow derived DC were incubated for 6 h with different concentrations of MPC6-32 in the presence (◆) or absence (■) of chloroquine (100 μM).

of exogenous antigens *via* the class II MHC pathway (*13*).

Remarkably, efflux of MPC6-32 **6** (Figure 2, panel e) and MPC6-40 **8** (Supplementary Figure 3) is extremely slow, with a half-life of over 3 h. Thus MPC6 appears to be continuously accumulated by the cell, with very little concomitant loss once uptake has occurred. Uptake of MPC6-32 **6** and MPC6-40 **8** is also strictly temperature-dependent and is blocked almost completely at 4 °C (Figure 2, panel f), consistent with a process requiring active internalization rather than simple equilibrium binding to a receptor. Uptake was also partly blocked in the presence of chloroquine (Figure 2, panel g), which inhibits intracellular acidification, consistent with a model in which MPC6 is taken into the cell *via* a receptor and then falls off the receptor at the acidic pH of the endosome.

As predicted, uptake involved a saturable interaction with the mannose residues of MPC6, since uptake could be competitively inhibited by excess mannosylated -BSA, but not by BSA alone (Figure 3, panel a). 50% inhibition of uptake required concentrations above 7.5 μM competitor, consistent with the relatively low affinity interaction between mannose receptors and their ligands (*14*). DC express a number of receptors of the lectin family, several of which can potentially bind mannose residues. Two lectin receptors which have received particular attention are DEC 205 (*15*) and the classical mannose receptor (*16*). Both are expressed on bone marrow de-

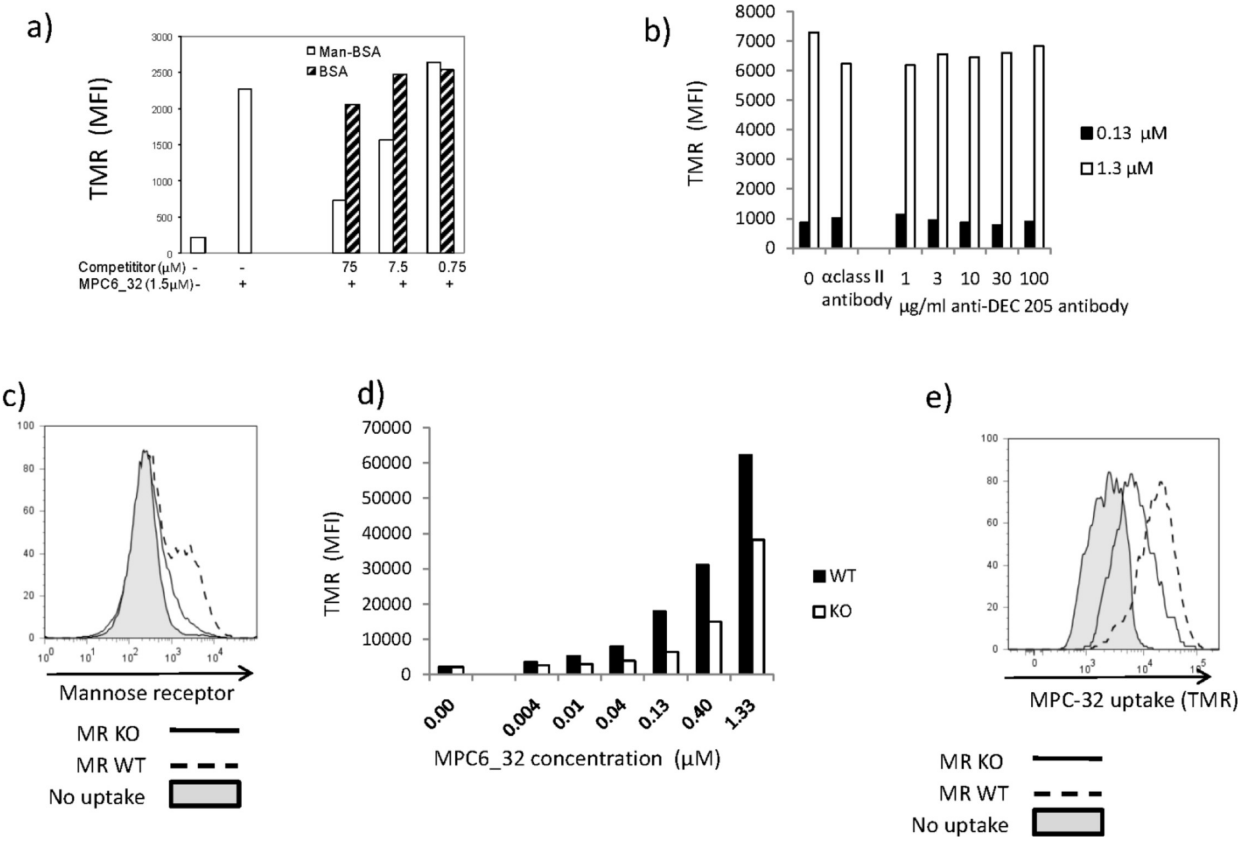

Figure 3. Uptake of MPC6 is mediated by mannose receptors. Uptake was analyzed by flow cytometry. Graphs show median fluorescent intensity (MFI) in the TMR channel. a) Competitive inhibition of MPC6 uptake. GM-CSF bone marrow derived DC (5×10^4) were cultured for 3 h at 37 °C in the presence of different concentrations of mannose-BSA or BSA. b) GM-CSF bone marrow derived DC (5×10^4) were cultured for 30 min in the presence or absence of different amounts of purified anti-DEC205 antibody (or as control an isotype matched anti-class II MHC antibody). MPC6-32 6 **(at high and low concentrations as shown) was then added for a further 3 h at 37 °C. c) Mannose receptor expression was detected by flow cytometry using a biotinylated antimannose receptor antibody and APC-streptavidin. d) Bone marrow derived DC from wild type and mannose receptor deficient mice were incubated in different concentrations of MPC6 for 3 h at 37 °C. e) A representative fluorescent histogram of the data in panel d, using a concentration of 0.13 μM MPC6-32** 6.

rived mouse DC. As shown in Figure 3, panel b), even very high concentrations of a monoclonal antibody to DEC205, NLDC145, which have been shown to block uptake of apoptotic cells *via* this receptor (*17*), were unable to block uptake of MPC6-32. This result is consistent with the structure of DEC205, which although belonging to the lectin family, lacks the classical mannose binding domains (*18*).

No blocking antibody to the classical mannose receptor has been described, so we were unable to carry out similar experiments to the above. However, we were able to compare uptake of MPC6-32 **6** in the presence and absence of this mannose receptor, using DC derived from mannose receptor deficient mice (Figure 3, panel c). As shown in Figure 3, panels d and e, uptake of MPC6-32 **6** was substantially lower in the absence of this receptor, particularly at lower concentrations, suggesting that this receptor has an important but not exclusive role in MPC-32 **6** uptake.

Distribution of MPC6 and Linker Stability within DC. Flow cytometry cannot readily distinguish between binding at the cell surface and uptake into the cell. The distribution of MPC6 within dendritic cells was therefore followed by confocal microscopy, using the fluorophore-labeled analogues of MPC6. Both MPC6-32 **6** and MPC6-40 **8** are seen clearly within the majority of DC.

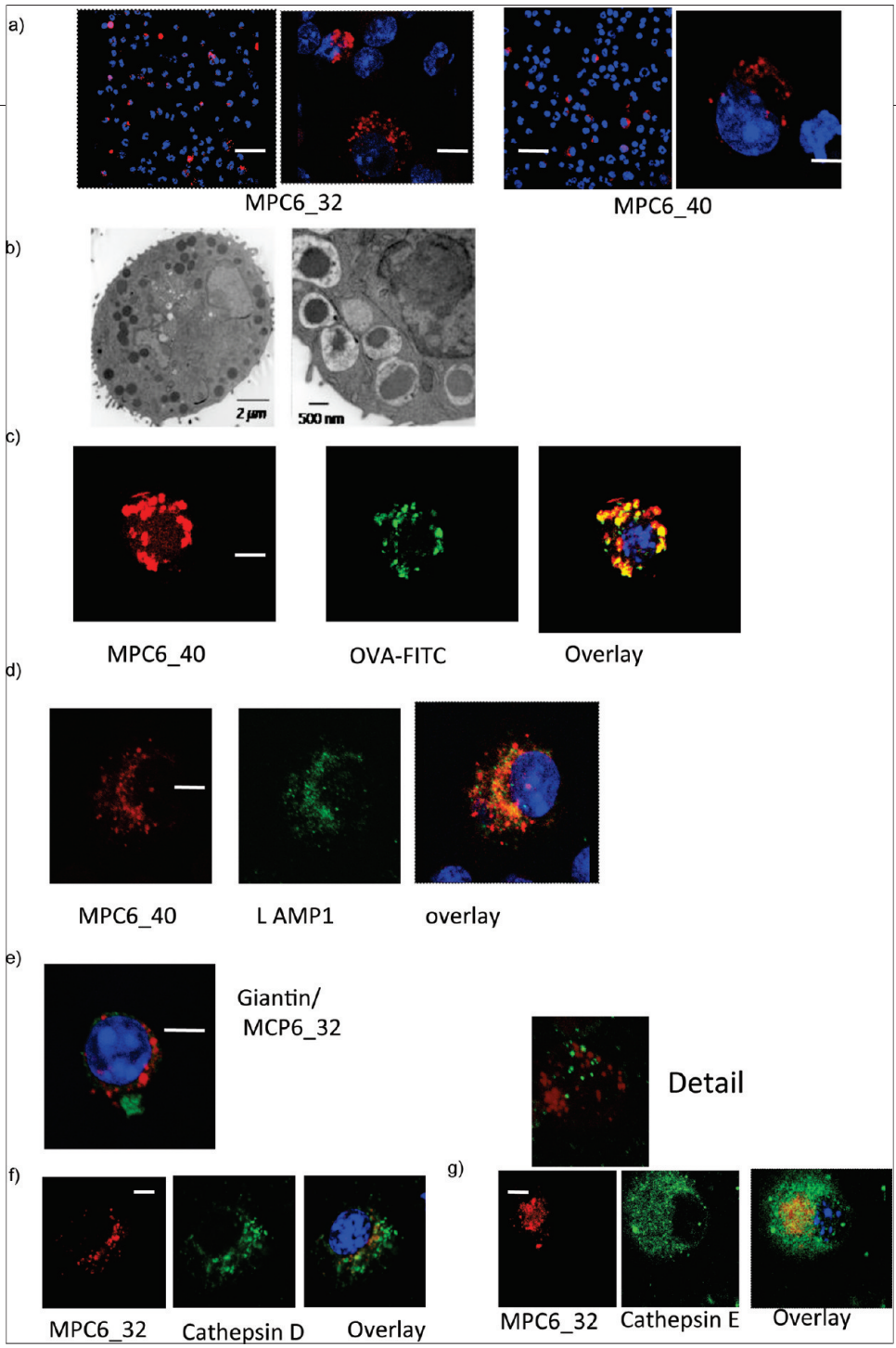

Figure 4. Intracellular localization of MPC6. a) GM-CSF bone marrow DC were incubated for 3 h in the presence of MPC6-32 6 (1 μM) and MPC6-40 8 (1 μM), washed, fixed, and processed for confocal microscopy. The panels show low (scale bar = 40 μm) and high (scale bar = 4 μm) magnifications showing the presence of intracellular labeled MPC6 in discrete vesicular structures. b) GM-CSF bone marrow DC were incubated for 3 h in the presence of MPC6-32 6 ((1 μM), washed, fixed, and processed for transmission electron microscopy. c) As for panel a, but OVA labeled with fluorescein isothiocyanate (FITC) (1 mg mL^{-1}) was added to the cultures 1 h prior to the end of the incubation period. Note the close overlay between OVA and MPC6 staining (scale bar = 4 μm). d–g) As for panel a, but cells were stained after fixation and permeabilisation using antibodies for the lysosomal protein LAMP 1 (d), the Golgi marker giantin (e), and the proteinases cathepsin D (f) and E (g) (scale bar = 4 μm).

The MPC6 derivatives are concentrated into vesicles of heterogeneous shape and size, often particularly densely packed in the perinuclear region, but fill a large proportion of the cytoplasmic volume in some cells (Figure 4, panel a). No obvious distinction could be observed between distribution of MPC6-32 **6** and MPC6-40 **8**, and for brevity the remaining panels each show only a representative image using one inhibitor.

In light of the size and extent of MPC6-containing vesicles observed by confocal microscopy, we also examined the ultrastructure of DC that had taken up unlabeled MPC6 by transmission electron microscopy (Figure 4, panel b). A number of DC from this group were indeed found to be packed with large electron dense vesicular structures, which sometimes filled a large proportion of the cytoplasm. The vesicles often contained a core of dense material, surrounded by less dense material. We hypothesize that within these structures MPC6 may form insoluble aggregates as it concentrates within endosomes, which may explain the extremely slow efflux observed in Figure 2, panel a.

Since previous studies had demonstrated inhibition of OVA processing by MPC6, the extent of co-localization of OVA and MPC6 was examined (Figure 4, panel c). OVA was taken up very efficiently by DC, and its distribution showed extensive co-localization with that of the MPC6 derivatives. Thus MPC6 successfully targets those endocytic compartments that also contain exogenous protein antigens taken up by DC.

The nature of the compartments was examined in more detail by immunofluorescent microscopy. MPC6 distribution overlapped significantly with LAMP1, a marker of late endosomes/lysosomes. However, a significant proportion of LAMP1 positive vesicles did not contain MPC6, confirming that lysosomes and endosomes are distinct compartments and that MPC6 has only partial access to the lysosomal system (Figure 4, panel d). As expected, MPC6 showed little overlap with the Golgi apparatus (Figure 4, panel e). The two targets of MPC inhibition within DC are the two aspartic proteinases cathepsin D and E. Cathepsin D is predominantly a lysosomal enzyme, and its distribution is similar to that of LAMP1. In contrast, cathepsin E is predominantly extralysosomal (*19*). As described previously (*6, 20*), its distribution is much more diffuse and reticular, and in contrast to the predominantly perinuclear distribution of cathepsin D, cathepsin E is also found at the cell periphery. MPC6 distribution showed significant overlap with both cathepsin D and E (yellow areas in Figure 4, panels f and g, respectively). However, some enzyme containing structures did not shown any MPC6 fluorescence. Interestingly, small cathepsin E containing vesicles were sometimes seen closely juxtaposed to but distinct from the much larger endocytic vesicles containing MPC6 (Figure 4, panel g, detail).

The design of MPC6 incorporates a disulfide bond containing linker. The rationale for this design was based on a considerable body of literature suggesting that the intracellular environment favors reductive cleavage of such disulfide-containing linkers (*8, 21*). We therefore hypothesized that cleavage of the disulfide linker of MPC6 would liberate pepstatin from the carrier and thus improve its bioavailability profile within the cell. However, the experiments shown in Figures 1−3 did not reveal much difference between the functional properties of MPC6-32 **6**, in which the fluorophore is attached to the BSA side of the linker, and MPC6-40 **8**, in which it is attached to the pepstatin side of the linker. Furthermore, a recent paper has questioned the hypothesis of a reductive endosomal environment (*22*).

We therefore tested the hypothesis directly, by synthesizing two analogues of MPC6-32, in which the TMR fluorescence is quenched by a QSY-9 group added to the other side of a linker. MPC6-98 **9** (Figure 5, panel a), containing a disulfide bonded linker equivalent to that in MPC6 between the TMR and QSY-9 groups, was again synthesized from **3** *via* selective deprotection, derivatization with QSY-9, and removal of the Fmoc group to give **10**. This was followed by formation of the iodoacetamide and conjugation to neomannosylated BSA to give **9** (Figure 5, panel a). As a control, the analogue MPC6-105 **11** (Figure 5, panel a), containing a simple aliphatic linker and resistant to reductive cleavage, was synthesized from 1,3-diaminopropane *via* a similar route (Supporting Information). For ease of synthesis, the pepstatin moiety was omitted from both quenched compounds.

Preliminary experiments demonstrated that the TMR-dependent fluorescence of MPC6-98 **9** increased 10- to 20-fold on reductive cleavage of the S−S bond with dithiothreitol, whereas in contrast MPC6-105 **11** was unaffected, confirming that the quenching was effective and could be reversed by cleavage of the disulfide bond. The uptake and fluorescence of both compounds by DC was then compared to that of MPC6-32, using flow cytometry (Figure 5, panel b). Unexpectedly, we could find no evidence of cleavage of MPC6-98 **9** even after 6 h of incubation with DC, and indeed there was no significant difference in emission between MPC6-98 **9** and MPC6-105 **11**. In order to reconcile the lack of linker cleavage with the observed potency of MPC6 in antigen processing and enzymatic functional assays, one must hypothesize that the pepstatin in MPC6 retains activity even when bound to linker and carrier. This hypothesis was tested by measuring the relative potency of MPC6 and pepstatin in cell free assays of cathepsin D and E inhibition. As shown in Figure 5, panel c, MPC6 was only about 2- to 3-fold less potent compared to free pepstatin, a decrease that may be accounted for by the incomplete coupling of pepstatin/linker to the BSA carrier as discussed above. Despite the attachment of a large carrier moiety, therefore, the pepstatin within MPC6 retains almost all its potency as a proteinase inhibitor.

Functional Inhibition of Aspartic Proteinase Activity by MPC6. Confocal microscopy demonstrated targeting of MPC6 to cathepsin D/E containing intracellular compartments. However, this approach cannot give quantitative information on the efficiency of enzymatic inhibition, particularly as the antibodies to the cathepsins do not distinguish between mature (active) enzyme and immature (inactive) precursor. Functional inhibition of aspartic proteinase activity by MPC6 was therefore assessed using two approaches. In the first, DC were

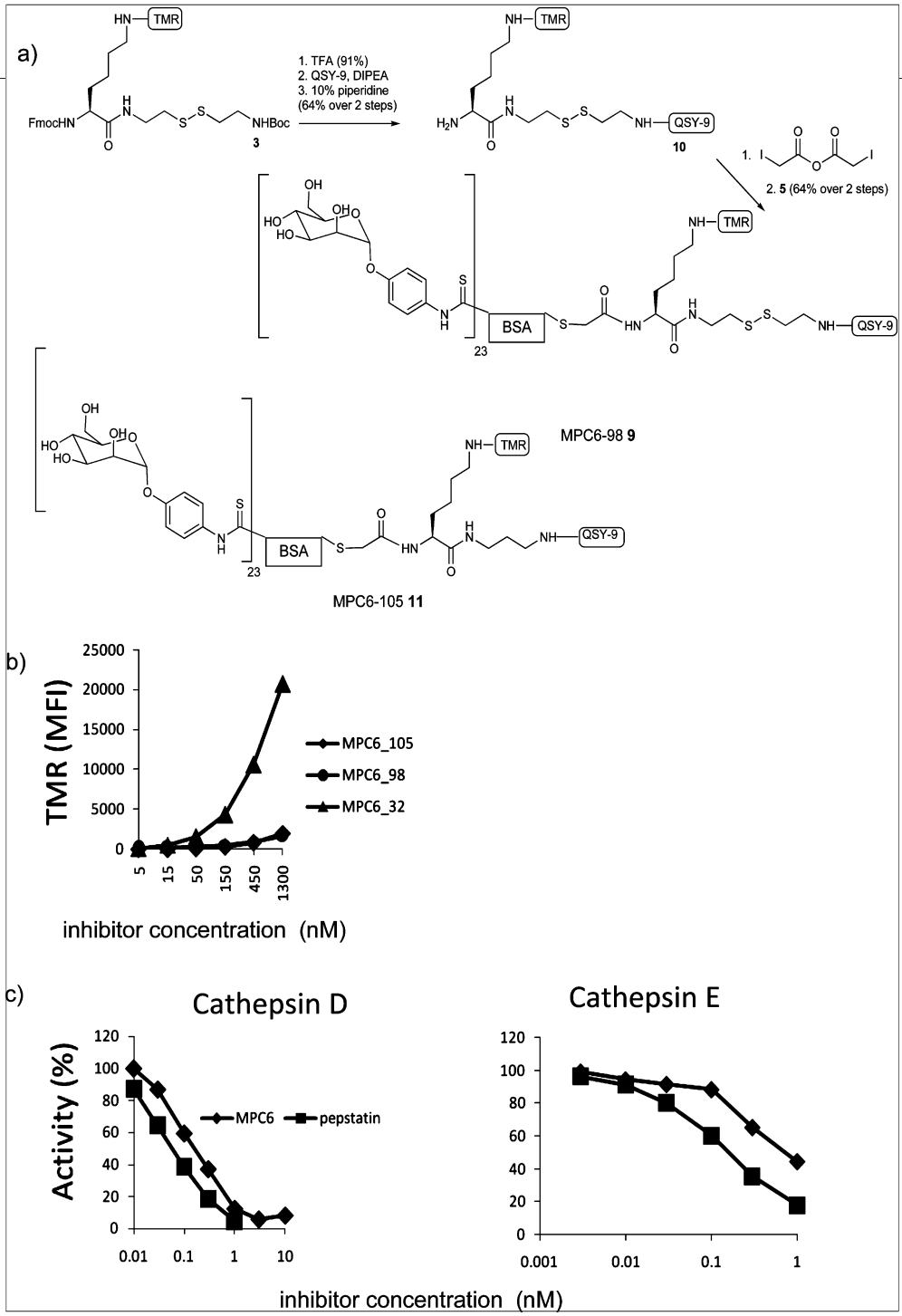

Figure 5. The role of disulfide bond cleavage in MPC6 activity. a) Scheme showing synthetic route to the quenched MPC6 analogue MPC6-98 9 **(containing a disulfide bond in the linker between the quencher QSY-9 and the TMR) and the structure of MPC6-105** 11 **(without this disulfide bond). b) The uptake of MPC6-98, MPC6-105, and MPC6-32 (*cf.* Figure 2, panel b) by GM-CSF bone marrow derived DC. The graph shows MFI of DC population after 6 h of incubation in presence of different compounds, plotted against compound concentration. c) The inhibition of cathepsin D and cathepsin E by MPC6 and pepstatin. Enzyme (1 nM) was incubated in the presence of inhibitor at the concentration shown and proteinase tested using a quenched fluorescent peptide substrate as described in Methods. The graph shows the activity as a percent of the activity in the absence of inhibitor.**

allowed to take up MPC6 for differing times and then lysed, and proteinase activity in the lysate at pH 4 was measured using a quenched fluorescein substrate that is efficiently cleaved by both cathepsin D and E (*23*) (Figure 6, panel a). In agreement with the uptake data shown in Figure 1, inhibition is both time- and dose-dependent. Levels of inhibition reached 60−70% at 10 μM MPC6 (the maximum tested), after exposure to MPC6 over 3−6 h. Addition of pepstatin after cell lysis inhibits over 95% proteinase activity (Figure 6, panel b), confirming that the assay is indeed selective for aspartic proteinase activity. Consistent with the very slow efflux of inhibitor observed, inhibition is long lasting, since cells that are allowed to take up MPC6 for 3 h, washed, and then incubated in the absence of inhibitor remain efficiently inhibited even after 18 h (Figure 6, panel c).

Activity of aspartic proteinases in DC was also measured using a flow cytometric assay, using the active site specific probe BODIPY-FL pepstatin (Figure 6, panel d). In this assay, DC are fixed and permeabilized at acidic pH and then incubated in the presence of BODIPY-FL pepstatin, in the presence or absence of excess pepstatin (*24*). Incubation of DC with MPC6 (10 μM) for 3 h resulted in 60−80% inhibition of specific binding of the active site probe. Furthermore, MPC6 inhibited BODIPY-FL pepstatin

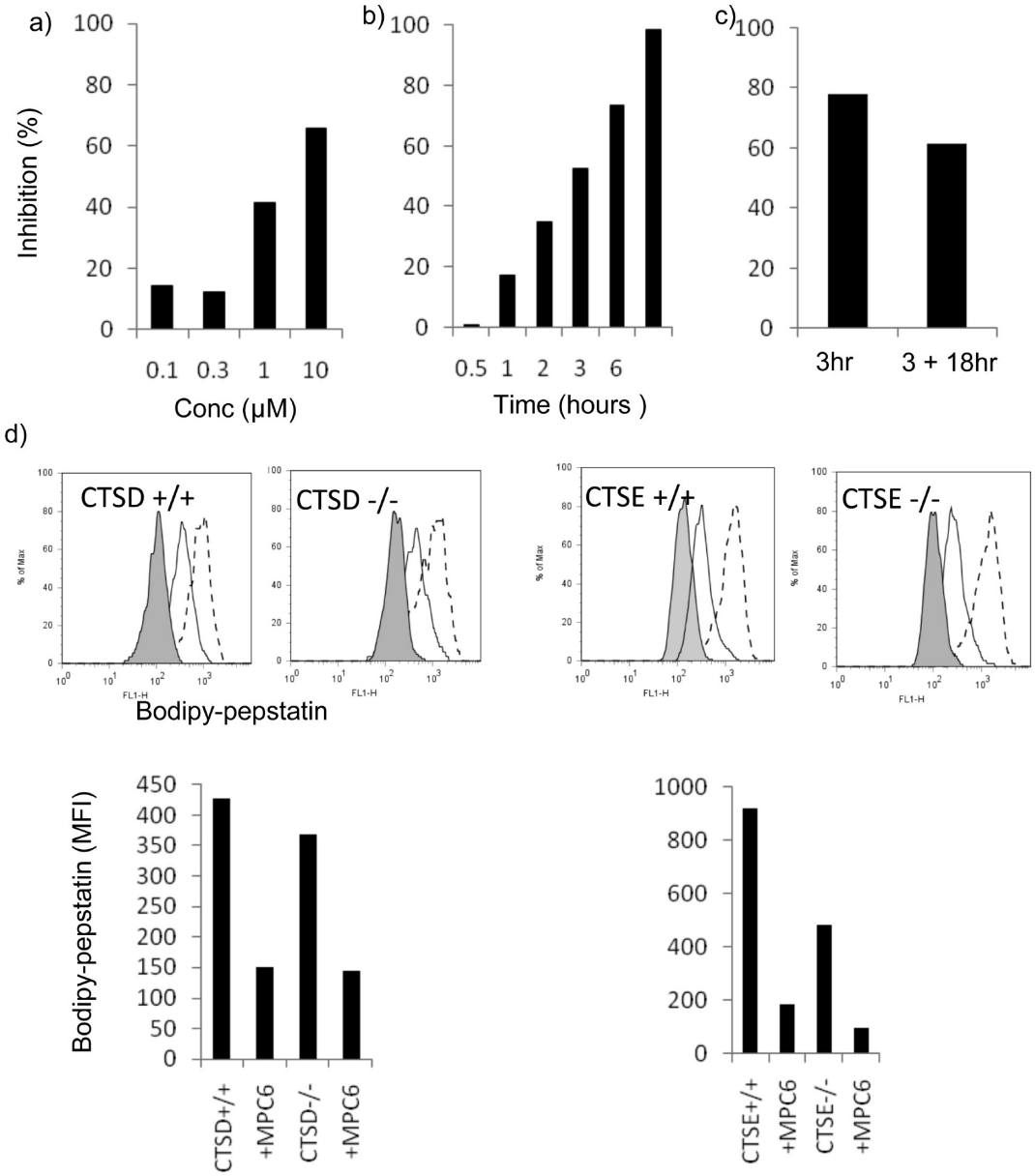

Figure 6. Inhibition of aspartic proteinase activity in DC incubated with MPC6. a) GM-CSF DC were incubated in the presence of different concentrations of MPC6 for 3 h. Excess MPC6 was removed by washing, the cells were lysed, and acid proteinase activity in 100 cell equivalents was measured as described in Methods. Results are expressed as percentage inhibition relative to activity of cells without inhibitor. b) GM-CSF DC were incubated in the presence of MPC6 (10 μM) for varying lengths of time. Cells were then washed, and proteinase activity was measured as in panel a. For the last unlabelled histogram, pepstatin (100 nM) was added after lysis. c) GM-CSF DC were incubated in the presence or absence of MPC6 (10 μM) for 3 h. Excess MPC6 was removed by extensive washing, a portion of cells was removed, and proteinase activity was measured as above (inhibition shown in column labeled 3). The remaining cells were incubated overnight in the absence of inhibitor, and proteinase activity was measured after a further 18 h of culture (column marked 3 + 18). d) GM-CSF DC from cathepsin D deficient (CTSD −/−), cathepsin E deficient (CTSE −/−), or wild type litter mate controls (CTSD +/+ and CTSE +/+) were incubated in the presence (solid line) or absence (dashed line) of MPC6 (10 μM) for 3 h, and aspartic proteinase activity was measured by staining with BODIPY-FL pepstatin as described in Methods. The filled histograms show fluorescent signal in the presence of excess unlabeled pepstatin (100 μM). The bar chart below the FACS profiles show MFI for each experimental group, after subtracting MFI in the presence of excess unlabeled pepstatin (100 μM).

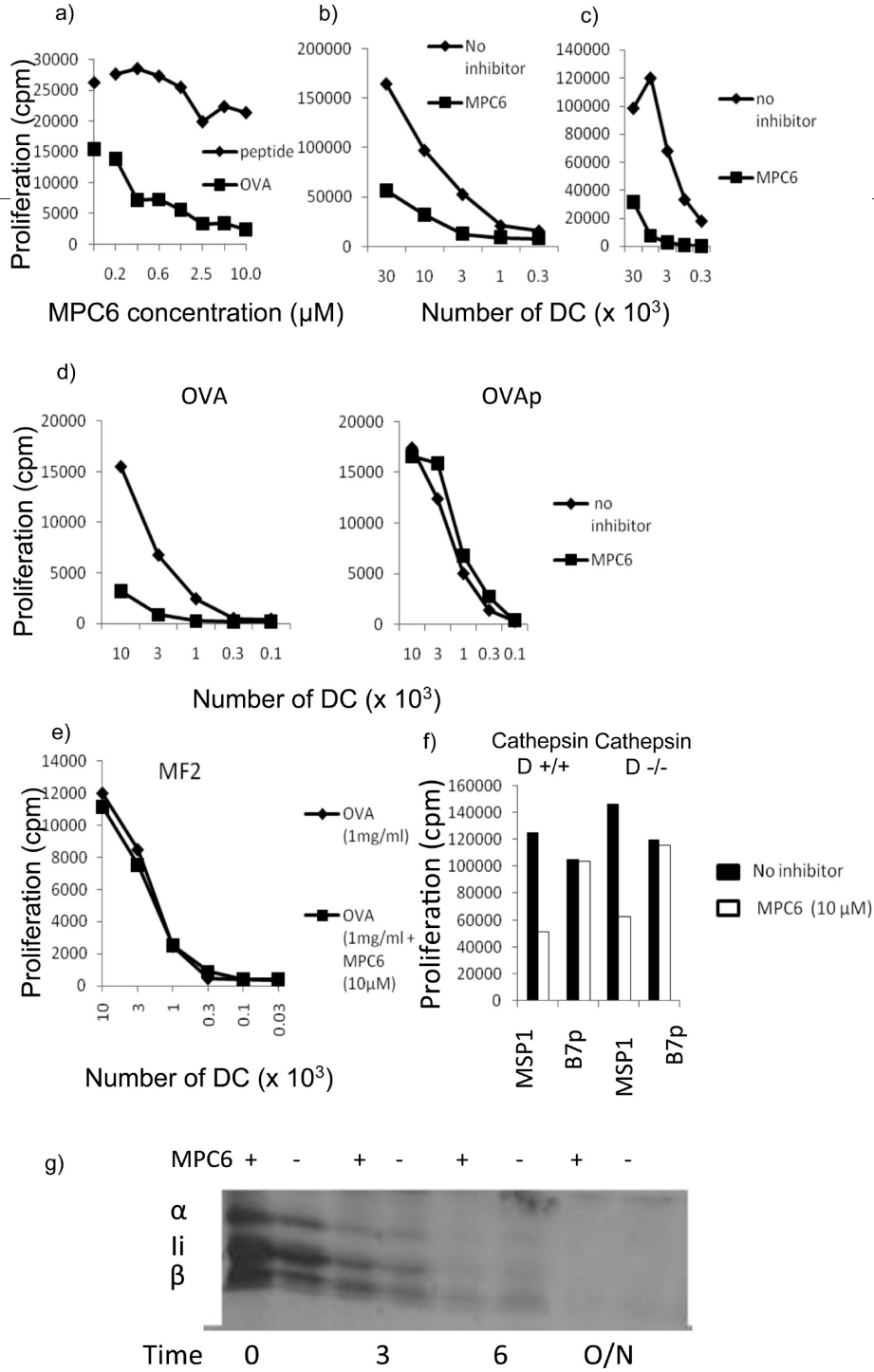

Figure 7. Inhibition of antigen processing in DC incubated with MPC6. a) GM-CSF DC (5000 cells) cultured from bone marrow of Balb/c mice were incubated with varying concentrations of MPC6 and co-cultured with ovalbumin (OVA, 1 mg mL^{-1}) or OVA peptide (323−339, 1 μg mL^{-1}), and the T cell hybridoma DO11.10 (2 × 10^4 cells). IL2 release was measured after 24 h. b) GM-CSF DC cultured from bone marrow of Balb/c mice were incubated with MPC6 (10 μM) for 1 h and then OVA (2 mg mL^{-1}) for a further 2 h. Excess OVA and inhibitor was removed by washing, and the cells were fixed with gluteraldehyde as described in Methods. Different numbers of fixed DC were then co-cultured with DO11.10 cells (2 × 10^4), and IL2 release was measured after 24 h. c) Splenic CD11c+ from Balb/c mice DC (105) were incubated with (■) or without (◆) MPC6 (10 μM) for 3 h and then co-cultured with OVA for a further 3 h. The DC were washed and co-cultured with DO11-10 cells as above. IL2 release was measured after 24 h. d) GM-CSF DC cultured from bone marrow of C57Bl mice were incubated with (■) or without (◆) MPC6 (10 μM) for 3 h and then co-cultured with OVA (left panel) or OVA peptide 323−339 (right panel) for a further 3 h. The DC were washed and co-cultured with OT-II transgenic T cells for 18 h. Proliferation was measured by thymidine incorporation. e) GM-CSF DC cultured from bone marrow of C57Bl mice were incubated with (■) or without (◆) MPC6 (10 μM) for 3 h and then co-cultured with OVA, and the T cell hybridoma MF2 (105 cells). IL2 release was measured after 24 h. f) GM-CSF DC cultured from bone marrow of cathepsin D deficient or wild type litter mates were incubated with or without MPC6 (10 μM), MSP1 protein, or MSP1 peptide (marked as B7p) and the B7 T cell hybridoma. IL2 release was measured after 24 h. g) GM-CSF bone marrow derived DC were pulsed labeled with S35 methionine in the presence or absence of MPC6 (10 μM) and then cultured for the times shown in the absence of label. Cells were lysed and immunoprecipitated with anti-Ii antibody In-1, and the immunoprecipitate fractionated by PAGE. Control immunoprecipitates using rat Ig showed no bands at the molecular weights of Ii or class I MHC.

binding equally both in DC from mice lacking cathepsin D and in DC from mice lacking cathepsin E. Thus MPC6 is able to target both cathepsin D and cathepsin E containing compartments in these DC.

The activity of MPC6 in inhibiting antigen processing of protein antigens is explored in Figure 7. Initial dose−response curves demonstrated that MPC6 maximally inhibited processing of OVA presentation to the specific T cell hybridoma DO11.10 but did not block antigen presentation of the synthetic peptide coding the OVA sequence 323−339, at concentrations of 10 μM (Figure 7a). This concentration was used in all subsequent experiments. In order to try and quantify the efficiency of blocking, DC were incubated with a fixed concentration of OVA and MPC6 and then fixed with gluteraldehyde to block further processing. Different numbers of DC were then co-cultured with DO11.10 cells (Figure 7, panel b). A comparison of dose responses in the presence or absence of inhibitor suggested that MPC6 increases the number of cells required to give an equivalent response by around 1 order of magnitude, consistent with a 90% decrease in number of OVA peptide/MHC complexes formed in the presence of the inhibitor. A similar dose response was observed using DC isolated directly from mouse spleen (Figure 7, panel c) rather than differentiated from bone marrow *in vitro*. DO11.10 is a rather insensitive T cell line, requiring 1−2 mg mL^{-1} OVA for efficient stimulation. We therefore tested MPC6 using OTII cells, TcR transgenic T cells recognizing the same peptide sequence of OVA but requiring 2−3 orders of magnitude less antigen (and presented by a different MHC class II haplotype). MPC6 showed similar levels of inhibition of processing of OVA in this model (Figure 7, panel d), confirming that the efficient inhibition observed was not specific to either the DO11.10 line used as indicator or the particular strain of MHC or mouse. The sensitivity of antigen processing to MPC6 was different for different epitopes. Thus no inhibition of processing was observed when using MF2 (Figure 7, panel e) or 3DO18.3 (Supporting Information Figure 4), two T cell lines that recognize a different portion of the OVA sequence. In contrast, MPC6 did inhibit processing of MSP1−19, a fragment of a protein from *Plasmodium chabaudi chabaudi* (*25, 26*) (Figure 7, panel f). Inhibition was not therefore a special feature of the single OVA epitope 323−339.

The exogenous class II MHC antigen processing pathway requires two proteolytic events, the cleavage of antigen into MHC-binding peptides and the cleavage of invariant chain, a protein that is associated with MHC in the ER and prevents binding until it is proteolytically degraded and removed. The proteinases responsible for Ii degradation remain poorly characterized (*27*), although early studies implicated aspartic proteinases (*28, 29*). It remained possible, therefore, that the effect of MPC6 could be attributed to its effect on invariant chain cleavage rather than a direct effect on antigen proteolysis. In order to assess this possibility directly, DC were loaded with MPC6, and invariant chain degradation followed by pulse-chase metabolic labeling and immunoprecipitation (Figure 7, panel g). At the concentrations that led to profound inhibition of antigen processing, MPC6 failed to block or retard invariant chain degradation.

***In Vivo* Targeting of DC by MPC6.** The selectivity of MPC6 was next examined *in vivo*, by injection of MPC6-40 **8** intravenously into mice. Mice were sacrificed after 3 h, and spleen cells isolated and analyzed by flow cytometry (Figure 8, panel a). An initial analysis of uptake on unfractionated spleen cells showed that MPC6-40 **8** was taken up by splenic CD11c positive DC (10−20% positive) but much less efficiently by lymphocytes (<5% positive). In order to analyze the specificity in more detail, CD11c cells were enriched by magnetic bead separation and the CD11b+ (myeloid) and CD11b− (lymphoid) cells (*30*) were analyzed separately (Figure 8, panel b). MPC6-40 **8** was found selectively in the myeloid (CD11b+) DC population and was inefficiently taken up by the CD11b DC. In agreement with this observation, MPC6-40 **8** could be detected in the CD11c+CD8− population (the equivalent of CD11b+) but not in the CD11c+CD8− population (Supplementary Figure 5). Significant staining was still observed 18 h after injection, although the levels were reduced compared to the 3 h time point.

The large molecular weight of MPC6 should limit access to nonlymphoid tissue *via* the endothelial blood vessel wall, but access of the inhibitor may occur at sites of inflammation when the barrier becomes more leaky. In order to test this hypothesis, mice were injected with MPC6-40 **8** intravenously, and peritoneal cells were collected either in unstimulated mice (Figure 8, panel c) or after inducing peritoneal inflammation by prior injection of thyoglycollate (*31*). The peritoneum contained lymphocytes, granulocytes, CD11b+CD11c− macrophages, and CD11b+CD11c+ DC. MPC6-40 **8** could not be detected in any population in unstimulated mice,

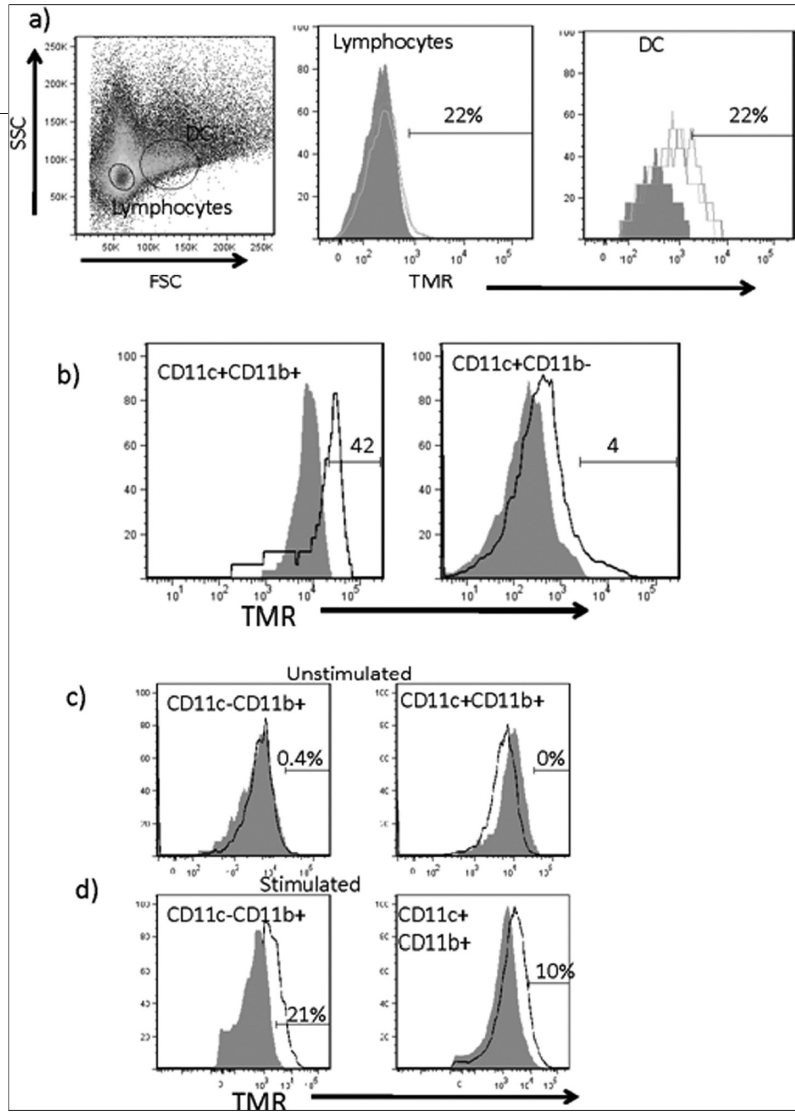

Figure 8. ***In vivo*** **targeting of MPC6. a) Mice were injected intravenously with 1 mg of MPC6-40 8 or left uninjected. Spleens were harvested after 3 h, and cells were stained for CD11c. The left panel shows the forward scatter/side scatter profile and the two gated populations. The smaller populations consisted of >98% lymphocytes; the larger population contained >90% of the total CD11c+ DC population. The left panel shows the MPC6-40 signal (measured as TMR fluorescence) for the lymphocytes and the CD11c+ DC, for control (shaded) and MPC6-40 injected mice (empty histograms). b) As for panel a, but the CD11c spleen cells were enriched by magnetic bead selection and then stained for CD11c and CD11b. The panels show the MPC6-40 signal (measured as TMR fluorescence) for the CD11b+CD11c+ DC and the CD11b−CD11c+ DC for control (shaded histogram) and MPC6-40 injected mice (empty histograms). One representative experiment of three. c) Mice were injected intravenously with 1 mg of MPC6-40 8 or left uninjected. Peritoneal exudates cells were harvested after 3 h, and cells were stained for CD11b and CD11c. The panels show the MPC6-40 signal (measured as TMR fluorescence) for the CD11b+CD11c− macrophages and the CD11b+CD11c+ DC for control (shaded histogram) and MPC6-40 8 injected mice (empty histograms). One representative experiment of three. d) As for panel c), but all mice received 2 mL of thioglycollate (3%) 3 days prior to the MPC6-40 injection. One representative experiment of three.**

confirming that the inhibitor did not cross the endothelium efficiently (Figure 8, panel c). In contrast, significant staining was observed in both macrophages and DC after thioglycollate (Figure 8, panel d).

CONCLUSION

This study describes the synthesis and functional properties of the inhibitor/carrier conjugate MPC6, which targets the aspartic proteinase inhibitor pepstatin to antigen presenting cells. A major goal of the study was to incorporate fluorescent groups into the basic structure that would allow efficient tracking of the conjugate by fluorescence microscopy or flow cytometry. The tetramethyl rhodamine (TMR) label chosen proved a good compromise between ease of chemical synthesis and good optical properties, allowing multiparameter analysis in combination with most of the commonly used fluorophores such as FITC, APC, and the PE-Cy5/7 tandem dyes. This approach therefore allowed tracking of MPC6 inhibitor within several subpopulations of heterogeneous cell mixtures both *in vitro* and *ex vivo*. This is a particularly important consideration in following DC targeting, since these cells are usually only a small minority of lymphoid tissue *in vivo* and consist of several subtypes with different function (*30*).

Using this fluorescent tracking approach, we demonstrated that MPC6 is avidly internalized by a variety of DC. Uptake was slow (compared, for example, to the very rapid binding of antibody conjugates to their target) and required micromolar concentrations of inhibitor. Both of these features, as well as the uptake block induced at 4 °C and the competitive block in the presence of BSA mannose, are compatible with a model of mannose-receptor facilitated uptake. DC express a number of receptors able to bind macromolecules containing mannose (*32*). The reduced uptake of MPC6 in the absence of the classical mannose receptor clearly demonstrates an important role for this receptor on bone marrow derived DC *in vitro*, but other members of the lectin family may well contribute *in vivo*. Further studies will be required to more precisely identify the contribution of each receptor on different DC and macrophage subsets *in vivo*.

The classical mannose receptor has a relatively low ligand binding avidity. However, low affinity reversible binding to a mannose receptor effectively increases the local concentration at the cell surface, leading to enhanced uptake *via* endocytosis (*33*). The ability to continually accumulate inhibitor over an 18 h period, the very slow efflux rates, and the sensitivity of the uptake to chloroquine further suggest that MPC6

does not remain bound to the receptor but dissociates at acidic endosomal pH, presumably allowing the receptor to recycle for further rounds of uptake. It remains unclear why MPC6 is not then lost from the cell, but a plausible hypothesis supported by the ultrastructural evidence of a large number of very electron-rich dense vesicles is that the high concentrations achieved within the endolysosomal compartment lead to aggregation, thus trapping the inhibitor within the cell. These properties of MPC6 require relatively high extracellular concentrations, for prolonged periods of time. However, the low affinity and hence reversible binding of MPC6 allows a recycling mechanism to occur, which can achieve very high levels of intracellular inhibitor. In contrast, antibody conjugate delivery depends on high affinity binding, which is fast and requires low concentrations of extracellular conjugate. However, the high affinity of the antibody−antigen interaction effectively means the interaction is irreversible, limiting uptake to the amount of antibody target present in the cell.

Confocal microscopy and enzymatic studies demonstrated that MPC6 is internalized to the antigen processing compartments of DC, which contain both internalized exogenous antigens and the two aspartic proteinases cathepsin D and E (*34*). Other compartments containing both proteinases clearly exist, presumably accounting for the fact that only partial inhibition of proteinase activity was achieved. The nature of this heterogeneity remains unclear, but both enzymes may be stored in storage vesicles (perhaps as proenzymes) and released into the appropriate endosomal compartment only upon appropriate stimulation. Such a regulated delivery model is compatible with the recent data (*35*) suggesting that efficient antigen processing occurs only in the presence of appropriate microbial stimulation.

An unexpected finding of our study was the apparent lack of role for the disulfide bond within the linker that joins the albumin and pepstatin portions of the conjugate. Using quenched fluorescent substrates, we were unable to find any evidence for substantial breakage of the linker within DC, even over a 6-h period. The inclusion of disulfide bond linkages in macromolecular drug delivery systems has become commonplace and is based on the widely held belief that the endosomal/lysosomal system provides a highly reductive environment, leading to cleavage of such linkers and release of active drug. The discovery of several specific enzymatic pathways for facilitating this S−S bond breakage (*8*) provided further apparent support for this model. However, relatively few studies have directly measured reductive cleavage of such linkers in situ. One recent study that did set out to measure cleavage also found no evidence for reduction within the endosomal system (*22*), whereas a second recent study demonstrated disulfide bond cleavage within endosomes (*21*). The reasons for these discrepancies remain unclear, although they may be related to the different cell types and receptor targeting used in the two reported studies. One further complexity is that disulfide bond cleavage may readily occur in the cytoplasm (which has a highly reductive environment) but disulfides in endosomes/lysosomes (which as shown by our confocal images are the major compartments targeted by MPC6) remain intact unless cleaved by specific enzymatic activity. In this regard, one important consideration is that the disulfide bond within the MPC6 linker does not have the same structure as the Cys−S−S−Cys bond found in natural protein disulfides and may therefore not act as an efficient substrate for the oxidoreductase enzymes such as GIILT that have been described within DC (*36*). Our work has also demonstrated that for MPC6 to function effectively as a targeted inhibitor of cathepsins D and E, dissociation of inhibitor and carrier may not be essential. This was also demonstrated in a recent study of targeting of cysteine proteases by mannose cluster-inhibitor conjugates in APCs (*37*). Further work on linker characterization may improve the susceptibility of conjugates to cellular reduction and hence improve the efficiency of delivery.

Despite the partial inhibition of proteinase activity and the lack of linker cleavage, MPC6 was remarkably efficient at blocking processing of OVA by DC. Comparison of DC dose−response curves suggested that MPC6 reduced the number of loaded MHC peptide complexes by as much as 90%. Thus MPC6 appears to effectively target the pool of aspartic proteinase, which is specifically required for antigen processing to occur. These studies support and extend our earlier studies proposing a nonredundant role for cathepsin E in the processing of OVA (*6*), although the relative importance of cathepsin D and E has not been further explored in the current study. The sensitivity of several other T cell epitopes to MPC6 inhibition was also explored. It is interesting that the two MPC6 sensitive epitopes OVA 323−339 and MSP1 1690−1709 are both within compact and proteolytically resistant domains of globular

proteins (*38*). In contrast, the two MPC6 resistant epitopes MF2 and 3DO18.3 T cells recognize epitopes that are exposed on the OVA protein surface. One may speculate that aspartic proteinase degradation may therefore be a specific requirement for releasing peptides from particularly resistant protein domains, although further work is required to test this hypothesis.

Finally, an important aspect of targeted delivery is the behavior of conjugates *in vivo*. This is especially important in the case of large molecular weight conjugates such as MPC6, since these molecules are unlikely to efficiently cross the endothelial barrier and therefore penetrate many tissues. MPC injected intravenously did indeed target spleen DC, consistent with the open blood supply to this organ. Uptake was selective, since very little MPC6-40 **8** could be detected in lymphocytes or CD11b−CD8+CD11c+ lymphoid DC, while fluorescence could readily be detected in CD11b+, CD8−, CD11c DC, which are the population principally involved in processing/presentation of exogenous antigens *via* Class II MHC to CD4+ T cells. Our preliminary results therefore suggest that the large size of MPC6, together with its tropism for antigen presenting cells, may paradoxically offer some benefits. Its size will prevent its access to most tissues, thus reducing any possible toxicities, but it will gain preferential access to immunologically active and/or inflammatory sites in which antigen presenting cells are typically most active, since these tissues typically show high endothelial permeability and accessibility. This hypothetic selective *in vivo* localization was confirmed using the classical inflammatory peritoneal model.

In conclusion, we have described a versatile modular approach to the synthesis of macromolecular carriers targeting inhibitors to the antigen presenting cell compartment of the immune system. The strategy has allowed us to incorporate diverse functional properties, including increased solubility in biological solutions, fluorescence at wavelengths suitable for tracking *via* confocal microscopy or flow cytometry, targeting *via* specific pattern recognition receptors, and delivery and accumulation within the endosomal intracellular compartment. These properties were achieved with little effect on the potency of the core inhibitor moiety pepstatin, and good inhibitory activity against the target antigen processing pathway. Targeted delivery *via* PRRs may therefore provide significant advantages for delivering high concentrations of immunomodulators to DC. Further modification of each element of the modular design will allow enhanced targeting selectivity, improved intracellular delivery, and delivery of a range of immunomodulators. Such targeted inhibitors will provide valuable tools for dissection of the immune system, as well as for delivering immunomodulators for prophylaxis or therapy.

METHODS

Details of chemical synthesis, purification and characterization, animals, culture media and cell isolations are all given in the Supporting Information.

***In Vitro* Uptake Experiments.** DC ($0.5-2 \times 10^5$/well) were cultured in the presence of MPC6-32, MPC6-40, MPC6-98, or MPC6-105 at 37 °C, 5% CO_2 for various times (15 min to 18 h) in a total volume of 200 μL of complete medium. The cells were washed twice in HBSS by centrifugation and then fixed in 3.8% formaldehyde. Fluorescence was analyzed on a FACSArray Bioanalyser (BD Biosciences). TMR fluorescence intensity was measured in the yellow channel. In some experiments, cells were processed for immunofluorescence prior to fixation. The cells were put on ice, and nonspecific binding was blocked by addition of 10 μL of rabbit serum for 10 min. Conjugated antibody (CD11c-PE (clone N418), CD11c-APC (clone N418), CD11c-PE-Cy7 (clone N418) or appropriate isotype controls, all purchased from BD Biosciences) diluted according to manufacturer's recommendations was added to each well and left for 45 min at 4 °C. The cells were washed twice in cold HBSS, fixed, and analyzed as above.

Mannose Receptor Studies. The anti-DEC205 antibody NLDC145 was purified from culture hybridoma supernatant by ammonium sulfate precipitation and DEAE-Sephadex ion exchange using standard methods. The hybridoma was obtained from Prof. Reis e Sousa, Cancer Research UK. Mannose receptor was visualized using a biotinylated anti-CD206 antibody (Cambridge Biosciences, no. 123003) and streptavidin-APC. The mannose receptor deficient mice have been described previously (*39*).

Confocal Microscopy. Dendritic cells were incubated in the presence of MPC6-32 **6** or MPC6-40 **8** (1 μM) for 3 h in CM. In some experiments, ovalbumin-FITC was added (1 mg mL^{-1}) for the last hour of incubation. The cells were washed in HBSS and 5×10^4 cells were allowed to adhere for 30 min on poly L-lysine (Sigma Aldrich, 100 μg mL^{-1} in water) coated 18 mm circular coverslips, at 4 °C. The cells were fixed for 10 min in 4% paraformaldehyde and mounted in DAPI containing mounting medium (Vectashield). In some experiments, the DC were further processed for immunofluorescence prior to mounting. After fixation in paraformaldehyde, DC were permeabilized in cold methanol (−20 °C) for 3 min (methanol rather than detergent permeabilization was found to be necessary in order to preserve localization of MPC6-32 and 40). The DC were washed in Tris-buffered saline (TBS), blocked in 20% goat or rabbit serum, and then stained with rabbit anti-LAMP1 (1:100 dilution in blocking

buffer, Abcam cat. no. ab24170), rabbit anti giantin (1:200 dilution in blocking buffer, Covance no. PRB-114C), goat anti anticathepsin D or goat anticathepsin E (1:20 dilution in blocking buffer, R&D) for 2−3 h. The coverslips were washed three times in TBS and then incubated in rabbit antigoat Ig FITC (DAKO) or goat antirabbit Ig FITC (DAKO) for 1 h, washed, and mounted as above. The images were collected and analyzed on a Leica confocal microscope, using Leica analysis software.

***In Vivo* Uptake Experiments.** Mice (with or without previous thioglycollate injection) were injected intravenously with 200 μL of MPC6-40 **8** (5 mg mL^{-1}) solution. Mice were sacrificed and spleens and/or peritoneal exudate cells were harvested after 3 or 18 h.

T Cell Presentation. Activation of the T cell hybridomas DO11.10 (OVA 323−339, I-A^d), MF2 (257−278, I-A^b) (kind gift of Dr. K. Rock, University of Massachusetts), and B7 (*Plasmodium chabaudi chabaudi* MSP1 1690−1709) was measured by assaying IL2 release as described previously (*25*). The MSP1 1−19 protein was prepared as described previously (*26*). Activation of T cells from the OTII TcR transgenic mouse (OVA 323−339, I-A^b) was measured by assaying for ^3H thymidine incorporation as described previously (*40*).

Antigen Processing Assay. DC were precultured in the presence of MPC6 for 30 min to 3 h (as detailed in figure captions) before addition of appropriate antigen and T cell (see above) for 18−24 h. In some experiments, antigen and inhibitor were removed by washing after a further 2 h of incubation and further antigen processing was blocked by fixation in 0.5% glutaraldehyde solution in phosphate buffered saline (PBS) (Sigma-Aldrich) for 30 s. Excess gluteraldehyde was quenched by adding an equal volume of complete medium, and the cells were washed twice. DC and T cell were then co-cultured for a further 18−24 h as above.

Invariant Chain Immunoprecipitation. Details in Supporting Information.

Proteolysis Assays. *Enzymatic.* Purified recombinant human cathepsin D (R&D) or E (R&D) or DC lysate was incubated in the presence of the specific aspartic proteinase quenched fluorogenic peptide substrate Mca-Gly-Lys-Pro-Ile-Leu-Phe-Phe-Arg-Leu-Lys(Dnp)-DArg-NH_2 (*23*) (200 μM, M-2455, Bachem) and buffer (1 M acetate, pH 4.0) for 10 min at 37 °C. Typically the incubation mixture contained 5 μL of substrate (final concentration 10 μM) and 10 μL of enzyme or lysate, 5−10 μL of inhibitor, and a total volume of 100 μL. The reaction was stopped by addition of 1 mL of cold trichloroacetic acid (5% w/v). Fluorescence was measured in a fluorimeter (Perkin-Elmer LS50B) set at excitation 328, emission 393. For measurement of enzymatic activity in DC (2×10^5) after incubation in the presence of MPC6, cells were washed three times to remove all exogenous inhibitor, and then lysed in 200 μL of 0.1% Triton-X in 0.15 M sodium acetate buffer, pH 4.5). The cell lysate was incubated for 15 min on ice, mixed, and then diluted further (1:10−1:50) in 0.15 M sodium acetate buffer, pH 4.5 without detergent. An aliquot of the diluted lysate was assayed as above.

Flow Cytometric. DC (2×10^5) were incubated for 3 h in the presence of MPC6 (10 μM). The cells were washed and fixed in 4% paraformaldehyde in 0.15 M sodium acetate buffer, pH 4.5. The cells were permeablized by adding an equal volume of Triton-X100 (0.2%, in 0.15 M sodium acetate buffer, pH 4.5) and then incubated with BODIPY-FL pepstatin (*24*) (500 nM final, InVitrogen) with and without excess pepstatin (100 μM) for 30 min at RT. The cells were washed twice with 0.15 M sodium acetate buffer, pH 4.5. Fluorescence intensity was measured by flow cytometry on a FACSCalibur (BD Biosciences). Specific aspartic protein dependent fluorescence is given by the difference in intensity between samples with and without excess unlabeled pepstatin. The fluorescence intensity was stable for at least 24 h.

Acknowledgment: The study was supported by the BBSRC (BB/D005469/1) under the SCIBS initiative. E.S. was supported by a MRC studentship. We are grateful to Professor N. Koch (University of Bonn) for the gift of antibodies for the invariant chain precipitation.

Supporting Information Available: This material is available free of charge *via* the Internet at http://pubs.acs.org.

REFERENCES

1. Trombetta, E. S., and Mellman, I. (2005) Cell biology of antigen processing *in vitro* and *in vivo*, *Annu. Rev. Immunol. 23*, 975–1028.
2. Shortman, K., Lahoud, M. H., and Caminschi, I. (2009) Improving vaccines by targeting antigens to dendritic cells, *Exp. Mol. Med. 41*, 61–66.
3. Frison, N., Taylor, M. E., Soilleux, E., Bousser, M. T., Mayer, R., Monsigny, M., Drickamer, K., and Roche, A. C. (2003) Oligolysine-based oligosaccharide clusters: selective recognition and endocytosis by the mannose receptor and dendritic cell-specific intercellular adhesion molecule 3 (ICAM-3)-grabbing nonintegrin, *J. Biol. Chem. 278*, 23922–23929.
4. Bedouet, L., Bousser, M. T., Frison, N., Boccaccio, C., Abastado, J. P., Marceau, P., Mayer, R., Monsigny, M., and Roche, A. C. (2001) Uptake of dimannoside clusters and oligomannosides by human dendritic cells, *Biosci. Rep. 21*, 839–855.
5. Free, P., Hurley, C. A., Kageyama, T., Chain, B. M., and Tabor, A. B. (2006) Mannose-pepstatin conjugates as targeted inhibitors of antigen processing, *Org. Biomol. Chem. 4*, 1817–1830.
6. Chain, B. M., Free, P., Medd, P., Swetman, C., Tabor, A. B., and Terrazzini, N. (2005) The expression and function of cathepsin E in dendritic cells, *J. Immunol 174*, 1791–1800.
7. Steinfeld, R., Reinhardt, K., Schreiber, K., Hillebrand, M., Kraetzner, R., Bruck, W., Saftig, P., and Gartner, J. (2006) Cathepsin D deficiency is associated with a human neurodegenerative disorder, *Am. J. Hum. Genet. 78*, 988–998.
8. Saito, G., Swanson, J. A., and Lee, K. D. (2003) Drug delivery strategy utilizing conjugation *via* reversible disulfide linkages: role and site of cellular reducing activities, *Adv. Drug Delivery Rev. 55*, 199–215.
9. Peters, T. (1996) *All about Albumin. Biochemistry, Genetics and Medical Applications*; Academic Press: New York.
10. Wilson, J. M., Wu, D., Motiu-DeGrood, R., and Hupe, D. J. (1980) A spectrophotometric method for studying the rates of reaction of disulfides with protein thiol groups applied to bovine serum albumin, *J. Am. Chem. Soc. 102*, 359–363.
11. Riener, C. K., Kada, G., and Gruber, H. J. (2002) Quick measurement of protein sulfhydryls with Ellman's reagent and with 4,4′-dithiodipyridine, *Anal. Bioanal. Chem. 373*, 266–276.
12. Naik, S. H., Proietto, A. I., Wilson, N. S., Dakic, A., Schnorrer, P., Fuchsberger, M., Lahoud, M. H., O'Keeffe, M., Shao, Q. X., Chen, W. F., Villadangos, J. A., Shortman, K., and Wu, L. (2005) Cutting edge: generation of splenic CD8(+) and CD8(−) dendritic cell equivalents in Fms-like tyrosine kinase 3 ligand bone marrow cultures, *J. Immunol. 174*, 6592–6597.
13. Sixt, M., Kanazawa, N., Seig, M., Samson, T., Roos, G., Reinhardt, D. P., Pabst, R., Lutz, M. B., and Sorokin, L. (2005) The conduit system transports soluble antigens from the afferent lymph to resident dendritic cells in the T cell area of the lymph node, *Immunity 22*, 19–29.
14. Benito, J. M., Gomez-Garcia, M., Mellet, C. O., Baussanne, I., Defaye, J., and Fernandez, J. M. G. (2004) Optimizing saccharide-directed molecular delivery to biological receptors: design, synthesis, and biological evaluation of glycodendrimer-cyclodextrin conjugates, *J. Am. Chem. Soc. 126*, 10355–10363.

15. Bonifaz, L., Bonnyay, D., Mahnke, K., Rivera, M., Nussenzweig, M. C., and Steinman, R. M. (2002) Efficient targeting of protein antigen to the dendritic cell receptor DEC-205 in the steady state leads to antigen presentation on major histocompatibility complex class I products and peripheral CD8+ T cell tolerance, *J. Exp. Med. 196*, 1627–1638.
16. McKenzie, E. M., Taylor, P. R., Stillion, R. J., Lucas, A. D., Harris, J., Gordon, S., and Martinez-Pomares, L. (2007) Mannose receptor expression and function define a new population of murine dendritic cells, *J. Immunol. 178*, 4975–4983.
17. Small, M., and Kraal, G. (2003) In vitro evidence for participation of DEC-205 expressed by thymic cortical epithelial cells in clearance of apoptotic thymocytes, *Int. Immunol. 15*, 197–203.
18. East, L., and Isacke, C. M. (2002) The mannose receptor family, *Biochim. Biophys. Acta 1572*, 364–386.
19. Zaidi, N., and Kalbacher, H. (2008) Cathepsin E: a mini review, *Biochem. Biophys. Res. Commun. 367*, 517–522.
20. Sealy, L., Mota, F., Rayment, N., Tatnell, P., Kay, J., and Chain, B. (1996) Regulation of cathepsin E expression during human B cell differentiation *in vitro*, *Eur. J. Immunol. 26*, 1838–1843.
21. Yang, J., Chen, H., Vlahov, I. R., Cheng, J. X., and Low, P. S. (2006) Evaluation of disulfide reduction during receptor-mediated endocytosis by using FRET imaging, *Proc. Natl. Acad. Sci. U.S.A. 103*, 13872–13877.
22. Austin, C. D., Wen, X. H., Gazzard, L., Nelson, C., Scheller, R. H., and Scales, S. J. (2005) Oxidizing potential of endosomes and lysosomes limits intracellular cleavage of disulfide-based antibody-drug conjugates, *Proc. Natl. Acad. Sci. U.S.A. 102*, 17987–17992.
23. Yasuda, Y., Kageyama, T., Akamine, A., Shibata, M., Kominami, E., Uchiyama, Y., and Yamamoto, K. (1999) Characterization of new fluorogenic substrates for the rapid and sensitive assay of cathepsin E and cathepsin D, *J. Biochem. (Tokyo) 125*, 113–1143.
24. Chen, C. S., Chen, W. N., Zhou, M., Arttamangkul, S., and Haugland, R. P. (2000) Probing the cathepsin D using a BODIPY FL-pepstatin A: applications in fluorescence polarization and microscopy, *J. Biochem. Biophys. Methods 42*, 137–151.
25. Quin, S. J., Seixas, E. M. G., Cross, C. A., Berg, M., Lindo, V., Stockinger, B., and Langhorne, J. (2001) Low CD4(+) T cell responses to the C-terminal region of the malaria merozoite surface protein-1 may be attributed to processing within distinct MHC class II pathways, *Eur. J. Immunol. 31*, 72–81.
26. Hensmann, M., Li, C., Moss, C., Lindo, V., Greer, F., Watts, C., Ogun, S. A., Holder, A. A., and Langhorne, J. (2004) Disulfide bonds in merozoite surface protein 1 of the malaria parasite impede efficient antigen processing and affect the *in vivo* antibody response, *Eur. J. Immunol. 34*, 639–648.
27. Maehr, R., Hang, H. C., Mintern, J. D., Kim, Y. M., Cuvillier, A., Nishimura, M., Yamada, K., Shirahama-Noda, K., Hara-Nishimura, I., and Ploegh, H. L. (2005) Asparagine endopeptidase is not essential for class II MHC antigen presentation but is required for processing of cathepsin L in mice, *J. Immunol. 174*, 7066–7074.
28. Mizuochi, T., Yee, S. T., Kasai, M., Kakiuichi, T., Muno, D., and Kominami, E. (1994) Both cathepsin B and cathepsin D are necessary for processing of ovalbumin as well as for degradation of class II MHC invariant chain, *Immunol. Lett. 43*, 189–193.
29. Kageyama, T., Yonezawa, S., Ichinose, M., Miki, K., and Moriyama, A. (1996) Potential sites for processing of the human invariant chain by cathepsins D and E, *Biochem. Biophys. Res. Commun. 223*, 549–553.
30. Shortman, K., and Liu, Y. J. (2002) Mouse and human dendritic cell subtypes, *Nat. Rev. Immunol. 2*, 151–161.
31. Griffin, F. M., Jr., Griffin, J. A., Leider, J. E., and Silverstein, S. C. (1975) Studies on the mechanism of phagocytosis. I. Requirements for circumferential attachment of particle-bound ligands to specific receptors on the macrophage plasma membrane, *J. Exp. Med. 142*, 1263–1282.
32. van Kooyk, Y. (2008) C-type lectins on dendritic cells: key modulators for the induction of immune responses, *Biochem. Soc. Trans. 36*, 1478–1481.
33. Levine, T. P., and Chain, B. M. (1992) Endocytosis by antigen presenting cells: dendritic cells are as endocytically active as other antigen presenting cells, *Proc. Natl. Acad. Sci. U.S.A. 89*, 8342–8346.
34. Medd, P. G., and Chain, B. M. (2000) Protein degradation in MHC class II antigen presentation: opportunities for immunomodulation, *Semin. Cell Dev. Biol. 11*, 203–210.
35. Blander, J. M., and Medzhitov, R. (2004) Regulation of phagosome maturation by signals from toll-like receptors, *Science 304*, 1014–1018.
36. Maric, M., Arunachalam, B., Phan, U. T., Dong, C., Garrett, W. S., Cannon, K. S., Alfonso, C., Karlsson, L., Flavell, R. A., and Cresswell, P. (2001) Defective antigen processing in GILT-free mice, *Science 294*, 1361–1365.
37. Hillaert, U., Verdoes, M., Florea, B. I., Saragliadis, N., Habets, K. L. L., Kuiper, J., Van Calenbergh, S., Ossendorp, F., van der Marel. G, A., Driessen, C., and Overkleeft, H. S. (2009) Receptor-mediated targeting of cathepsins in professional antigen presenting cells, *Angew. Chem., Int. Ed. 48*, 1629–1632.
38. Babon, J. J., Morgan, W. D., Kelly, G., Eccleston, J. F., Feeney, J., and Holder, A. A. (2007) Structural studies on *Plasmodium vivax* merozoite surface protein-1, *Mol. Biochem. Parasitol. 153*, 31–40.
39. Lee, S. J., Evers, S., Roeder, D., Parlow, A. F., Risteli, J., Risteli, L., Lee, Y. C., Feizi, T., Langen, H., and Nussenzweig, M. C. (2002) Mannose receptor-mediated regulation of serum glycoprotein homeostasis, *Science 295*, 1898–1901.
40. Tulone, C., Tsang, J., Prokopowicz, Z., Grosvenor, N., and Chain, B. M. (2007) Natural cathepsin E deficiency in the immune system of C57BL/6J mice, *Immunogenetics 59*, 927–935.